



## Designing a sub-wavelength array to change the direction of the radiation wave to a desired angle using variable Huygens surfaces

Sajedeh Zamani Noughabi<sup>1</sup>, Amir Saman Nooramin\*<sup>1</sup>, Mohammad Soleimani<sup>1</sup>

Department of Electrical Engineering, The Iran University of Science and Technology (IUST), Tehran, Iran

**ABSTRACT:** Since Huygens structures with phase shift lead to beam rotation, this manuscript discusses a phase shifter structure for the Huygens surface based on Tapered Slot Transition in the frequency range of 9.95-10.2 GHz using varactor diodes. By inducing an electric field along the tracks and placing diodes, the phase can be changed up to 200 degrees. With unit cells of 0.2  $\lambda_0$  -that this size is the smallest possible size for beam rotation structures - and a mega cell of 4 unit cells, incident angles of 0-15 degrees can be converted to transmitted angles of 10-45 degrees. The unit cell has been fabricated and it is shown that the measurement results are in good agreement with the simulation one.

### Review History:

Received: Jun. 22, 2024

Revised: Aug. 25, 2024

Accepted: Nov. 29, 2024

Available Online: Nov. 29, 2024

### Keywords:

Varactor Diode

Beam Rotation

Radiation Angle

Huygens Surface

### 1- Introduction

The design and realization of tunable meta-surfaces face fundamental challenges due to strict requirements on phase coverage, impedance matching, and loss [1]. These structures find many applications in phased array antenna, intelligence surface, and ... by creating arbitrary electromagnetic wave fronts through field discontinuities [2]. Tunable metasurfaces offer numerous degrees of freedom by changing the phase responses of each Unit cell individually using active elements [3]. However, achieving these poses challenges in maintaining phase coverage, impedance matching, and ensuring high efficiency[1], [2],[3].

Huygens' metasurfaces are sub-wavelength structures that can induce electric and magnetic dipole moments when illuminated by a radiation field. The smaller dimensions of the Huygens unit cell compared to metasurfaces allow for more accurate design based on surface impedances and admittances, which ensures higher efficiency of wave transmission and higher phase coverage. However, one of the main challenges in Huygens plates is their narrow radiation angle, which can limit the efficiency of the structure[1], [4], [5].

Tapered slot transition structures have been utilized in [6] and [7] as spatial power amplifiers within the waveguide or when connecting the waveguide to microstrip lines. These structures offer several advantages, including high efficiency,

low loss, and increased variation due to their adjustable unit cell phase. The planar phase shifter structure of tapered slot transition structures can be integrated with various beam rotation platforms, demonstrating their excellent application prospects.

In this manuscript, a subwavelength adjustable phase shifter has been implemented using a Tapered slot transition structure. Phase tuneability has been implemented based on the voltage of the varactor diodes. In fact, by applying a suitable DC bias to the varactor diodes placed in each microcell, the phase required to rotate the beam for input angles of 0 to 15 degrees to any arbitrary output angle in the range of 20 to 45 degrees is provided. The operating bandwidth is [9.9, 10.2] GHz.

The structure of single cells and megacells, as well as suitable phases for beam rotation to desired angles, are discussed in Section 1. In Section 2, beam rotation and simulation of unit cells are examined. Section 3 focuses on the single cell measurement setup and presents measurement and simulation results with this test setup.

### 2- Design unit cell and mega cell

The value of the phase gradient  $\frac{d\phi}{dx}$  during the length of the unit cell, needed to rotate the input beam with radiation angle  $\theta_i$  to the output angle  $\theta_r$  at wavelength  $\lambda_0$ , is calculated from Eq. (1), which represents the generalized Snell's law of refraction. In this equation,  $n_t$  and  $n_i$  are the refraction coefficients of the incident and transmitted

\*Corresponding author's email: A\_nooramin@iust.ac.ir



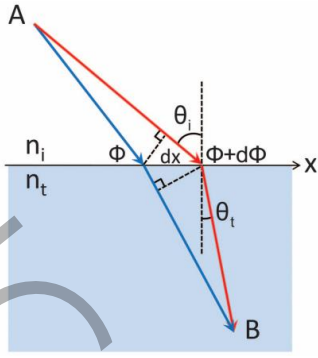


**Fig. 1. Schematics used to derive the generalized Snell's law[8]**

wave medium, respectively [8]. Furthermore,  $\theta_i$  and  $\theta_t$  are the angles of incident and transmitted wave, respectively, in regards to the surface normal, as shown in Fig. 1.

$$\sin(\theta_t)n_t - \sin(\theta_i)n_i = \frac{\lambda_0}{2} \frac{d\phi}{dx} \quad (1)$$

Based on Eq. 1, and what is mentioned above, Table 1 shows the required phase difference between two adjacent unit cells for several incident and beam rotation angles.

The structure of the unit cell is based on the Rogers 4003C substrate with a height of 0.508mm, as shown in Fig. 2(a). As shown in this figure, the parameters of the structure are depicted. All the dimensions are detailed in Table 2. In general, the structure consists of 3 parts. First, the wave is almost linearly coupled to the slot lines, then the wave is propagated inside the structure and the appropriate phase shift is applied to it. The design includes a curved and

tapered line to facilitate the better coupling of X-polarized waves. The diodes are placed where the maximum surface current is induced on the line shown in Fig 2(e). The use of triangular grooves on a structure aims to reduce the capacitive impedance of the main structure by adding a varactor diode. This concept is illustrated in Fig. 2(d) and shows the equivalent impedance of triangular and rectangular grooves. By changing the capacitance  $C_2$ , the resonance frequency and resulting magnitude of  $s_{21}$  will change.

Fig3 .(a), (b), and (c) shows the magnitude of  $s_{21}$  in terms of frequency for different lengths of the rectangular groove, the length of the triangle, and the width of the unit cell. It is shown the optimal values for each parameter.

The Varactor diode SMV1430-040LF by SkyWorks is used in the single-cell simulation, employing the Floquet Port boundary conditions in Ansys Electronics Desktop HFSS 2021R2 software where the incident wave is radiated downward to the structure, as shown in Fig. 2(c). The simulation results are depicted in Fig. 3

### 3- The Simulation of Beam Rotation

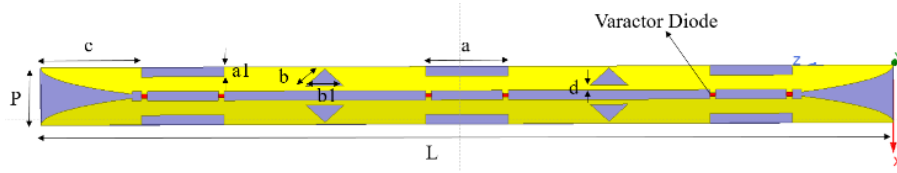
The maximum phase difference required to convert a beam with an incident angle of  $0^\circ$  to a transmission angle of  $45^\circ$  that a phase difference of 50 degrees between two adjacent unit cells is required as shown in Table 1. This means that placing 4 unit cells in a megacell requires that a single cell can provide at least  $150^\circ$  of phase difference so that 4 single cells can be placed together in a megacell with  $50^\circ$  of phase difference between each one.

This simulation has been done as shown in Fig 2(c) for different values of the bias voltage and the achieved results of magnitude of  $s_{21}$ , phase of  $s_{21}$ , and magnitude of  $s_{11}$  are shown in Fig. 4(a), Fig 4(b), and Fig. 4(c), respectively. As shown in this Fig, the phase difference of 198 degrees can be reached at 10 GHz and above 160 degrees from 9.95-10.2 GHz. Table 3 shows a comparison with the previously performed beam rotation and phase changer structures.

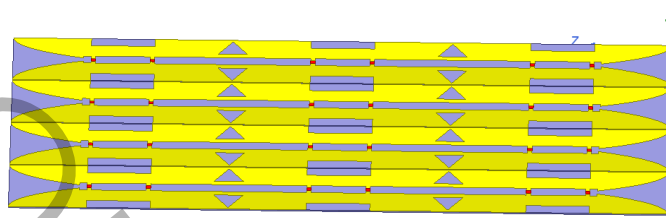
The question pertains to the placement of a diode within

**Table 1. Value and unit of the parameter structure**

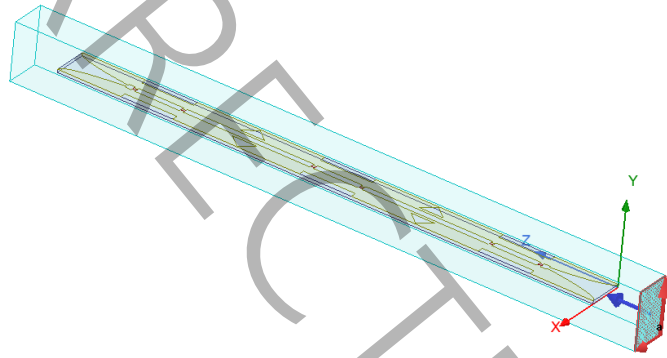
Incident Angle [deg]	Beam Rotation Angle [deg]	The required phase difference between two adjacent Unit cells [deg]
0	45	50.9
0	30	36
0	20	24.6
10	45	46.4
15	45	43.7
10	30	33.7



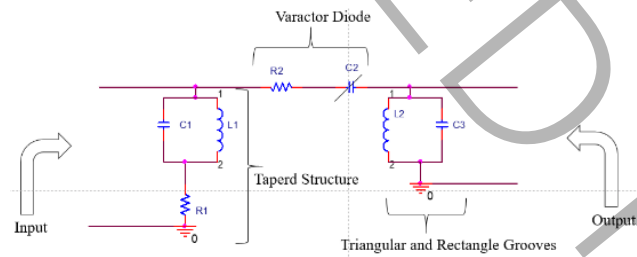
(a)



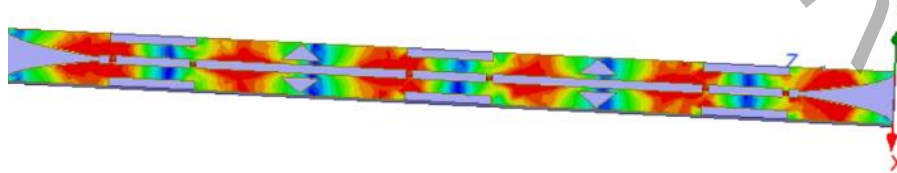
(b)



(c)



(d)

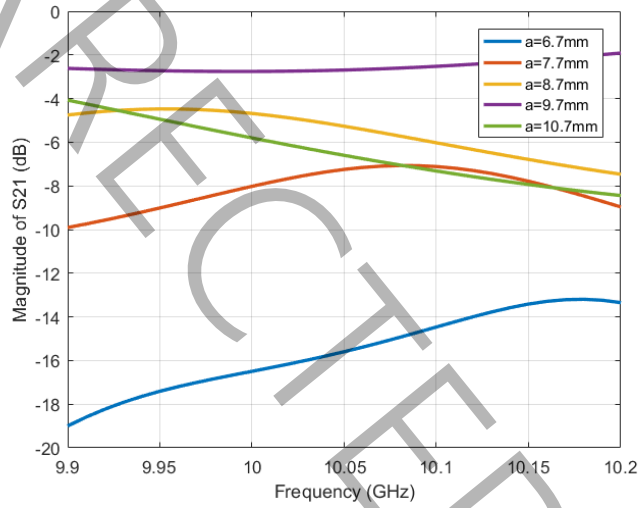


(e)

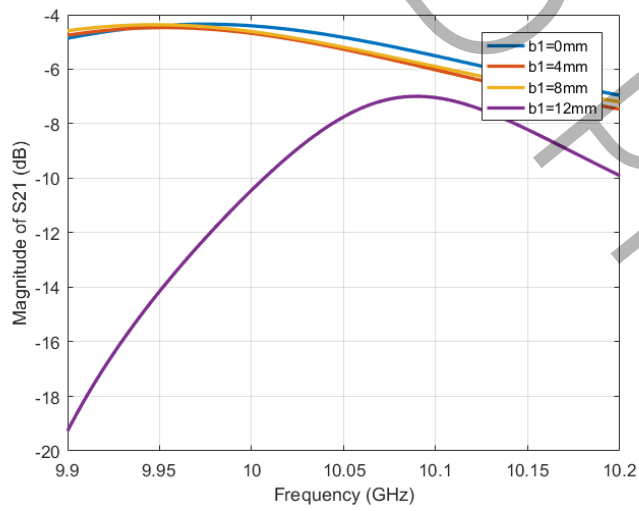
Fig. 2. Structure of (a) Unit cell. (b) Megacell. (c) Floquet Port simulation. (d) Equivalent Circuit of the Unit cell and (e) Surface current in the Unit cell.

**Table 2. The dimentions in the Uni cell**

Parameter	Dimension (mm)	Dimensions in terms of $\lambda$
$P$	6	0.2
$L$	90	3
$a$	8.7	0.29
$a_1$	1	0.001
$b$	2.69	0.089
$b_1$	4	0.13
$c$	10.65	0.355
$d$	0.5	0.006



(a)



(b)

**Fig. 3. Analysis parameter of the Unit cell (a) a (b)  $b_1$  and (c) P in bias voltage is 4 V.(Continued)**

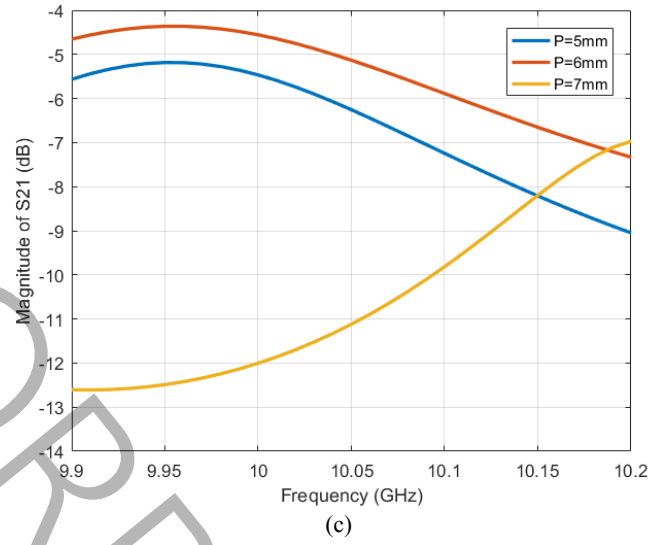


Fig. 3. Analysis parameter of the Unit cell (a)  $a$  (b)  $b_1$  and (c)  $P$  in bias voltage is 4 V.

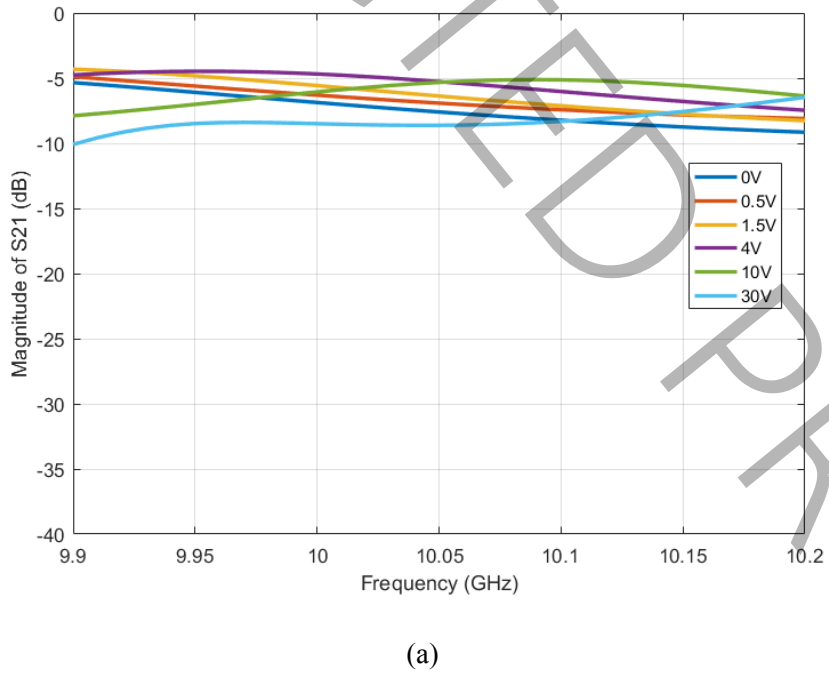
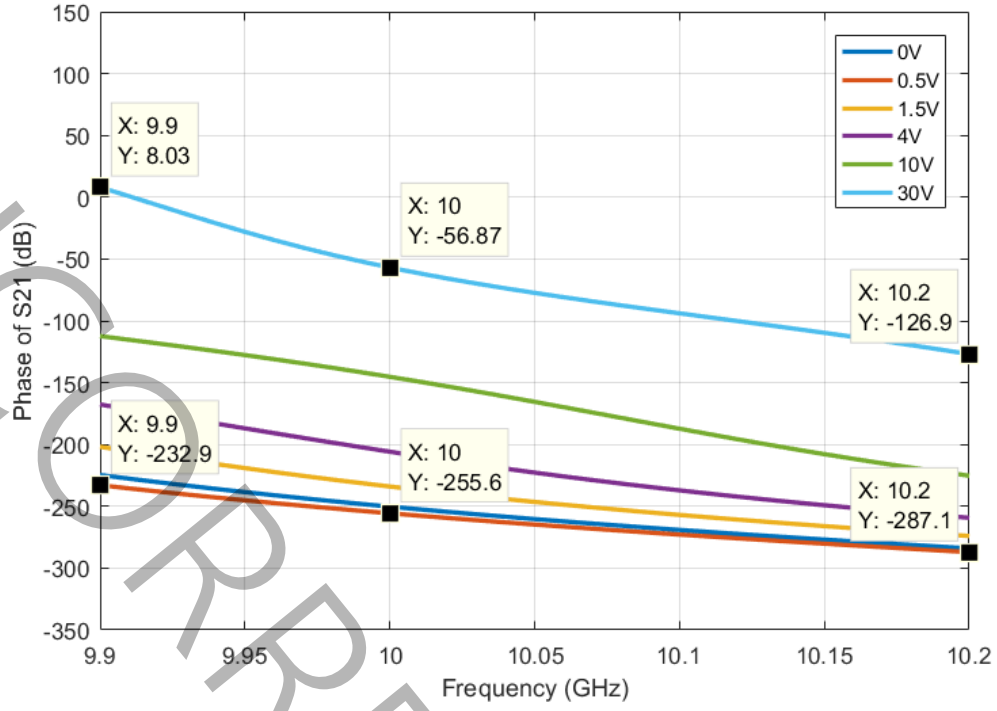
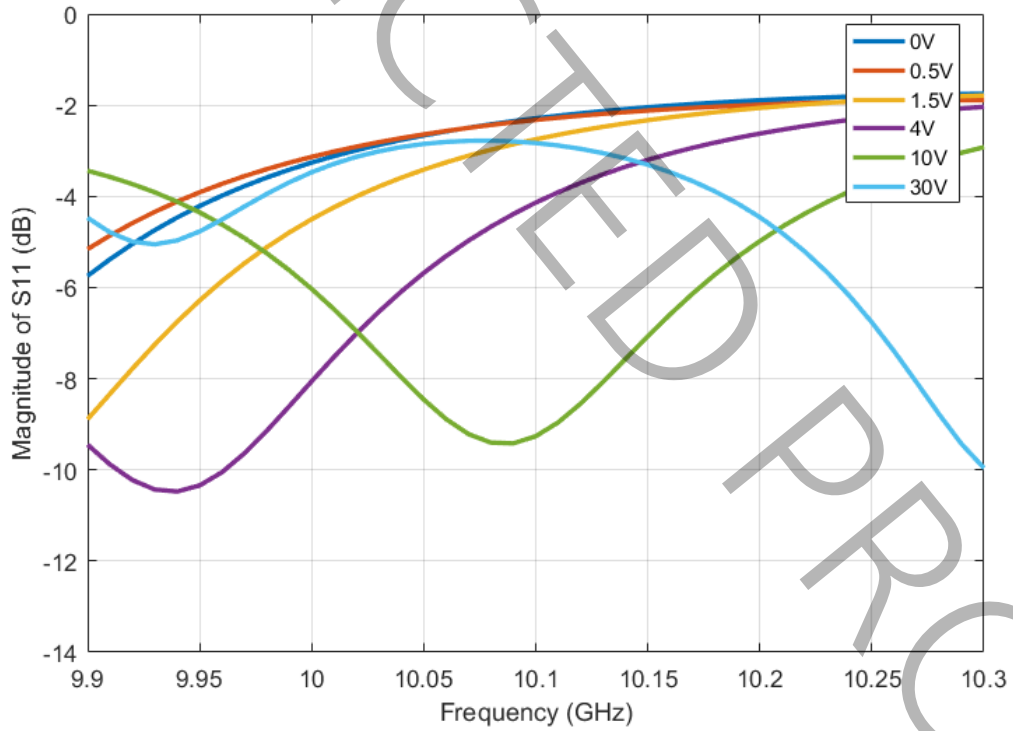


Fig. 4. AThe results of Unit cell simulation for different diode bias voltage (a) Magnitude of  $s_{21}$ . (b) Phase of  $s_{21}$  and (c) Magnitude of  $s_{11}$ .(Continued)



(b)

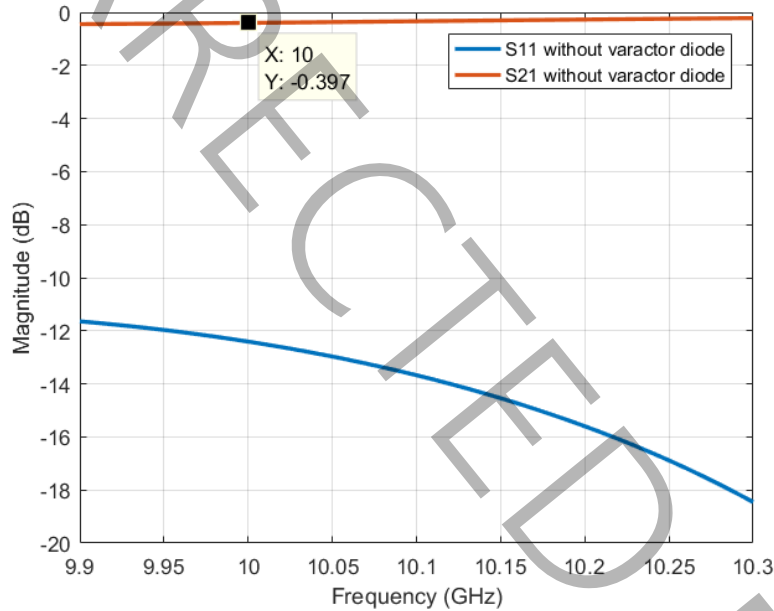


(c)

Fig. 4. AThe results of Unit cell simulation for different diode bias voltage (a) Magnitude of  $s_{21}$ . (b) Phase of  $s_{21}$  and (c) Magnitude of  $s_{11}$ .

**Table 2. The dimentions in the Uni cell**

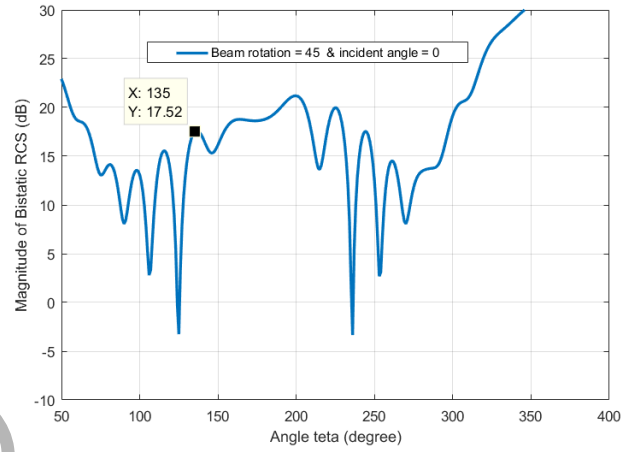
Reference	Bandwidth / $f_0$	Phase Shift	Dimension of Unit Cell	Type
[9]	400 MHz / 24.5 GHz	270°	$0.24 \lambda \times 0.24 \lambda$	Reflection with Varactor Diode
[10]	- / 3.5 GHz	145°	$0.3 \lambda \times 0.3 \lambda$	Reflection with Varactor Diode
[11]	1 GHz / 2.5 GHz	193°	With lump element	
This Work	250 MHz / 10 GHz	198° in Simulation and 145° in Measurement	$0.2 \lambda \times 3 \lambda$	Transmission with Varactor Diode

**Fig. 5. Result of simulation Unit cell without Varactor diode.**

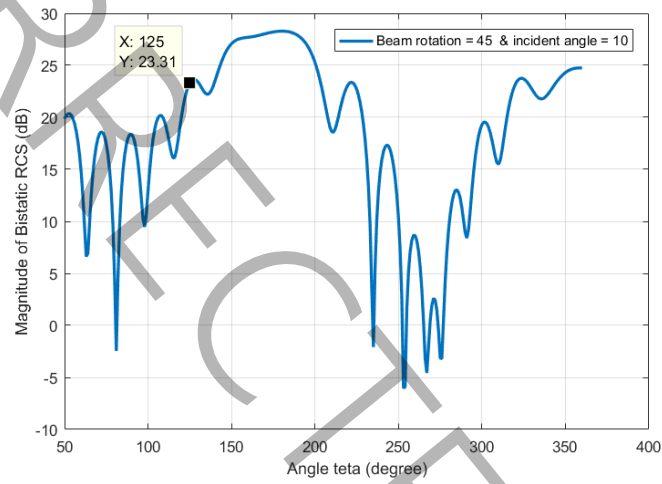
a structure and its impact on wave reflection due to non-ideal diode characteristics. The scattering parameters of the structure without a diode are plotted in Fig. 5 to validate this issue and it shows a low loss and match structure. To observe the rotation of the beam, a bistatic radar cross-section is used. The beam rotation simulation results for various angles can be observed in Fig. 6 which peaks at the expected angle. To rotate the beam with an input angle of 0 degrees and transfer it to a transmission angle of 45°, the diagram should have a peak value at an angle of 135° (the transmission angle on the opposite page  $135 = 45 - 180$ ) and similarly, for the rest of the angles shown in Fig. 6, this argument is valid.

#### 4- Test Setup and measurement results

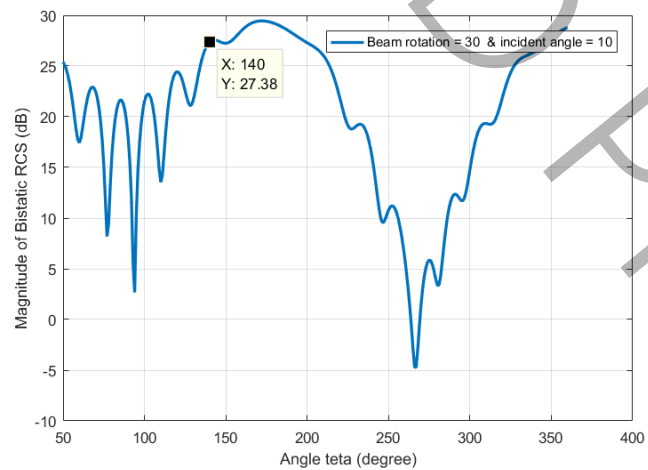
The unit cell test setup involves a standard X-band waveguide WR-90 to provide the necessary boundary conditions for periodic simulation. This setup ensures that the field is parallel to the diode in the structure (in the X direction) the vertical electric field above and below the structure is equal to zero and in the middle is maximum on the unit cell. By utilizing the waveguide, conditions similar to a Floquet port can be established. The simulation results of the transmitted wave in the unit cell inside the waveguide for various diode varactor bias voltages are depicted in Fig. 8. This approach allows the accurate evaluation of the unit cell's



(a)



(b)



(c)

**Fig. 6. Result of beam rotation in Megacell (a) 0-degree incident to 45 degree transmit. (b) 10 degree incident to 45 degree transmit and (c) 10 degree incident to 30 degree transmit degree.**



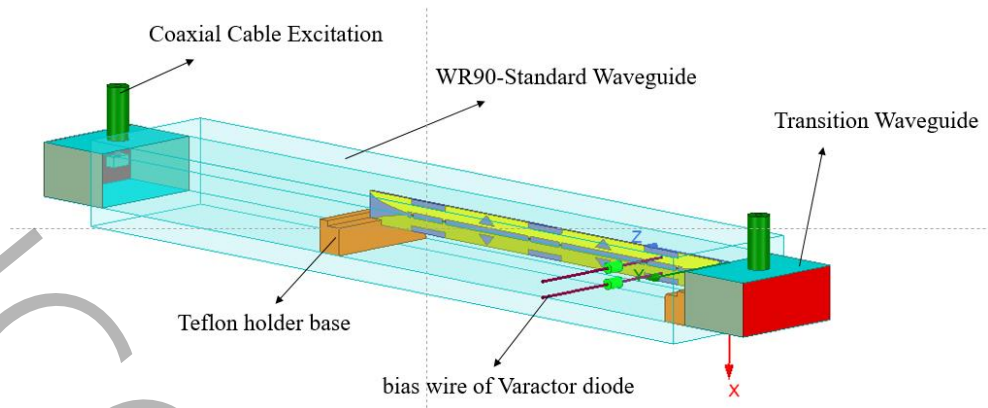
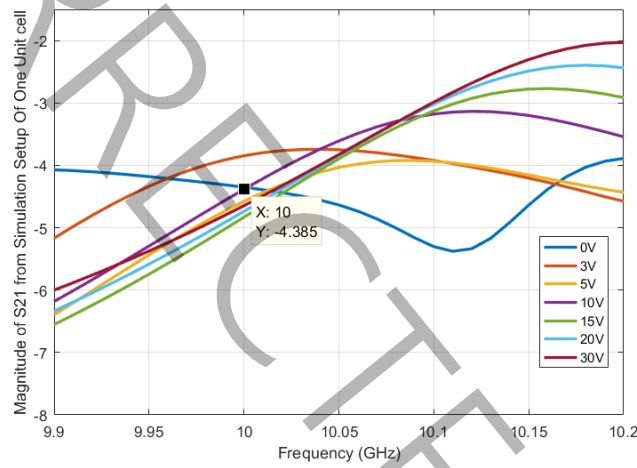
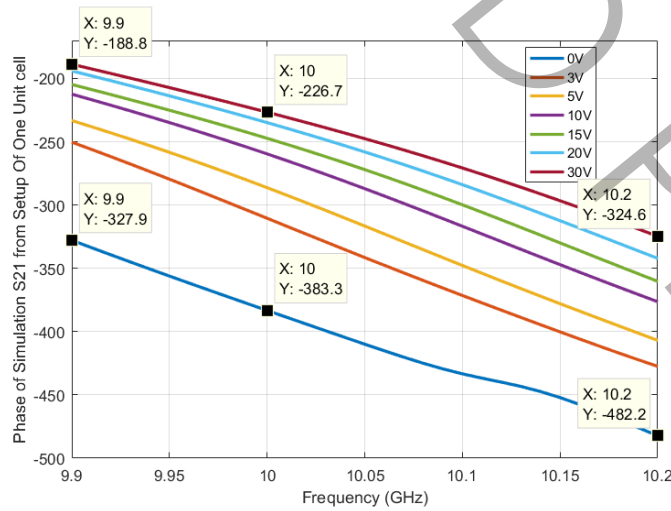


Fig. 7. Setup of one Unit cell.



(a)



(b)

Fig. 8. Result of simulation Unit cell waveguide Setup (a) Magnitude and (b) Phase  $S_{21}$  for a different bias voltage of Varactor diode.

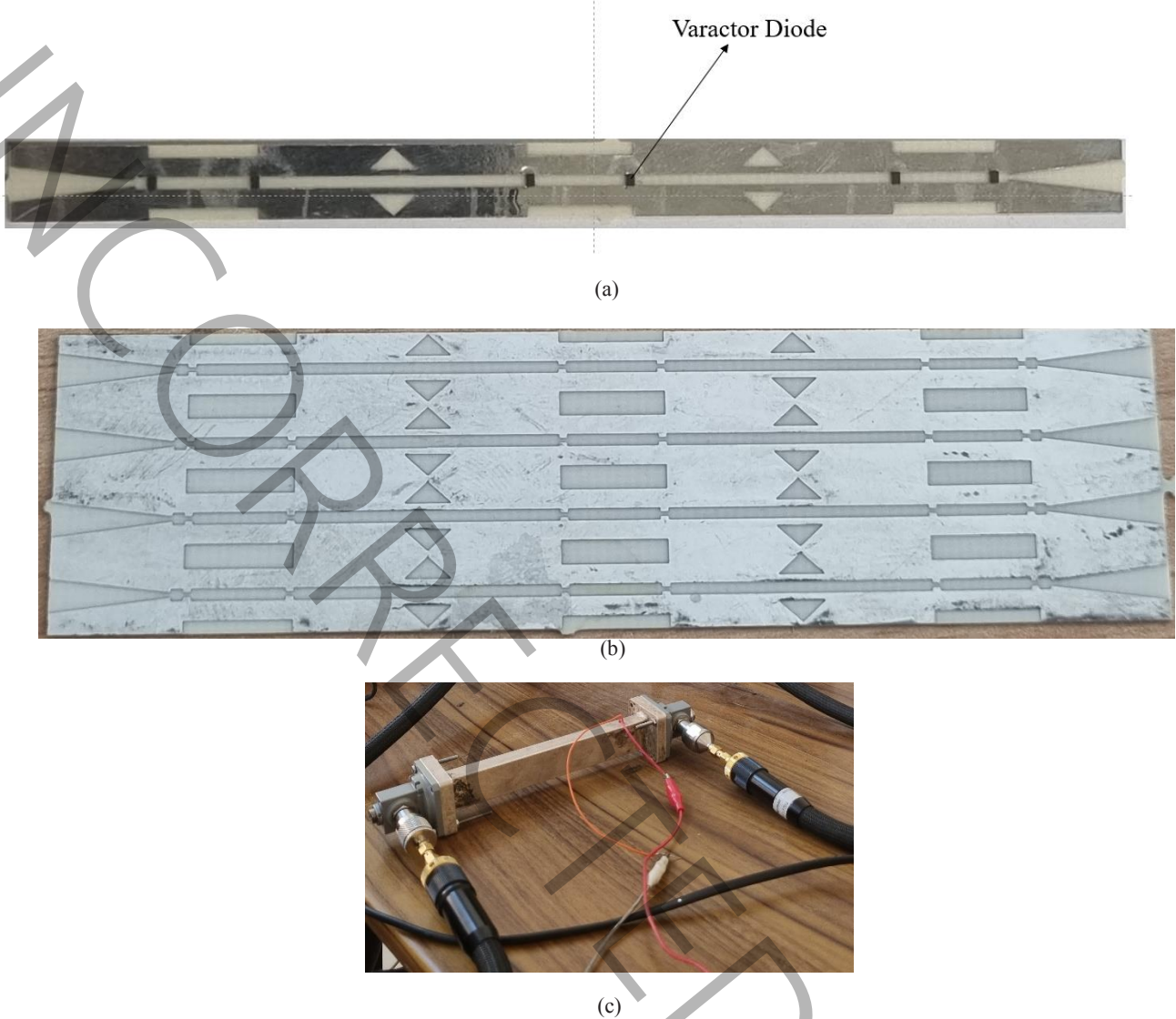


**Fig. 9.(a) A fabricated unit cell with diodes assembled on it. (b) fabricated Megacell without diode and (c) the test Setup of the unit cell.**

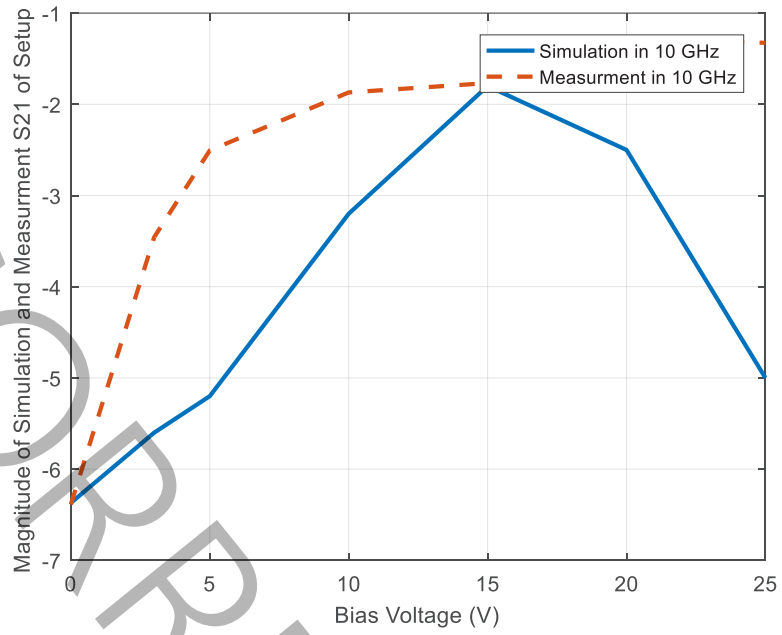
performance under different bias voltages. A phase difference of  $156^\circ$  can be reached as shown in Fig. 8(b).

The fabricated unit cell and the test setup are depicted in Fig. 9(a) and 9(c), respectively. The magnitude and phase of  $s_{21}$  from measurement and simulation results of are illustrated in Fig. 10(a) and 10(b) respectively.

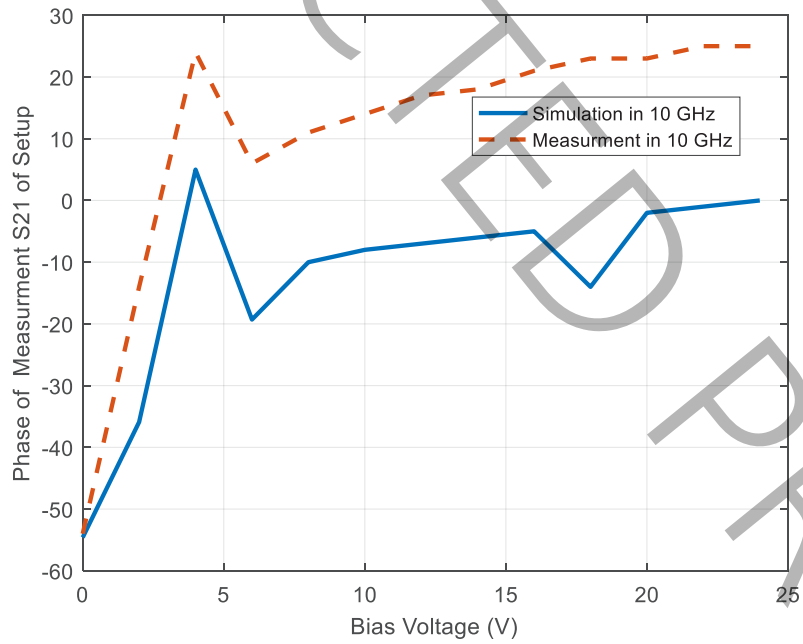
As shown in Fig 10(b), the phase starts from  $-45^\circ$  for 0 V bias voltage and reaches  $24^\circ$  at 4 V, and remains the same at 6 V. Subsequently, at 6 V, the phase value is  $6^\circ$  and increases thereafter. The phase transitions from 0 V to 4 V, to  $-180^\circ$  changes, then the phase becomes positive and starts of  $24^\circ$ . Ultimately, the phase difference obtained from the measurement results is  $145^\circ$ , indicates a high level of agreement between simulation and measurement.

### 5- Conclusion

The article discusses a Unit cell structure of the Tapered Slot Transition type that can change the phase by adjusting the voltage bias of the vector diode within it. This structure offers advantages for beam rotation applications compared to Huygens and Metasurface structures due to its simplicity of construction and smaller dimensions, approximately  $0.2 \lambda$ , aiding in reducing the side lobe level and grating lobe. The study presents the result of beam rotation for various radiation angles up to  $15^\circ$  and transmission angles ranging from  $10^\circ$  to  $45^\circ$ . Additionally, the structure can be expanded by combining 4 single cells to create a megacell. The phase change results of this constructed structure validate the simulation accuracy and highlight the potential applications



(a)



(b)

Fig. 10.(a) Result of measurement and simulation (a) Magnitude and (b) Phase of  $S_{21}$  .

of this unit cell in various fields.

### References

- [1] K. Chen et al., "A Reconfigurable Active Huygens' Metalens," arXiv:1702.01920, vol. arXiv:1702.01920, 02/07 2017, doi: 10.1002/adma.201606422.
- [2] J. Tang, S. Xu, F. Yang, and M. Li, "Design and Measurement of a Reconfigurable Transmitarray Antenna With Compact Varactor-Based Phase Shifters," IEEE Antennas and Wireless Propagation Letters, vol. 20, no. 10, pp. 1998-2002, 2021, doi: 10.1109/LAWP.2021.3101891.
- [3] Q. He, S. Sun, S. Xiao, and L. Zhou, "High-Efficiency Metasurfaces: Principles, Realizations, and Applications," Advanced Optical Materials, vol. 6, 2018.
- [4] V. Ataloglou and G. V. Eleftheriades, Arbitrary Wave Transformations with Huygens' Metasurfaces through Surface-Wave Optimization. 2021.
- [5] Y. Wang et al., "Huygens' Metasurface With Stable Transmission Response Under Wide Range of Incidence Angle," IEEE Antennas and Wireless Propagation Letters, vol. 21, pp. 630-634, 03/03 2022, doi: 10.1109/LAWP.2022.3140749.
- [6] L. Valletti, S. Fantauzzi, and F. Di Paolo, "An Innovative Lens Type FinLine to Microstrip Transition," Journal of Infrared, Millimeter and Terahertz Waves, vol. 43, 09/01 2022, doi: 10.1007/s10762-022-00869-z.
- [7] X. Shan, "Study of spatial power combining in closed waveguides," Doctor of Philosophy, School of Electrical & Electronic Engineering, Nanyang Technological University, 2013.
- [8] N. Yu et al., "Light Propagation with Phase Discontinuities: Generalized Laws of Reflection and Refraction," Science (New York, N.Y.), vol. 334, pp. 333-7, 09/01 2011, doi: 10.1126/science.1210713.
- [9] L. Silva, Z. Chu, P. Xiao, and A. Cerqueira S. Jr, "A varactor-based 1024-element RIS design for mm-waves," Frontiers in Communications and Networks, vol. 4, 03/22 2023, doi: 10.3389/frcmn.2023.1086011.
- [10] S. Tian, H. Liu, and L. Li, "Design of 1-Bit Digital Reconfigurable Reflective Metasurface for Beam-Scanning," Applied Sciences (Switzerland), vol. 7, 08/28 2017, doi: 10.3390/app7090882.
- [11] G. Chaudhary and Y. Jeong, "Wideband Tunable Differential Phase Shifter With Minimized In-Band Phase Deviation Error," IEEE Microwave and Wireless Components Letters, vol. 29, no. 7, pp. 468-470, 2019, doi: 10.1109/LMWC.2019.2920270.

#### HOW TO CITE THIS ARTICLE

S. Zamani Noughabi, A. S. Nooramin, M. Soleimani. Designing a sub-wavelength array to change the direction of the radiation wave to a desired angle using variable Huygens surfaces. AUT J. Elec. Eng., 57(1) (2025) 43-54.

DOI: [10.22060/ej.2024.23291.5599](https://doi.org/10.22060/ej.2024.23291.5599)

